

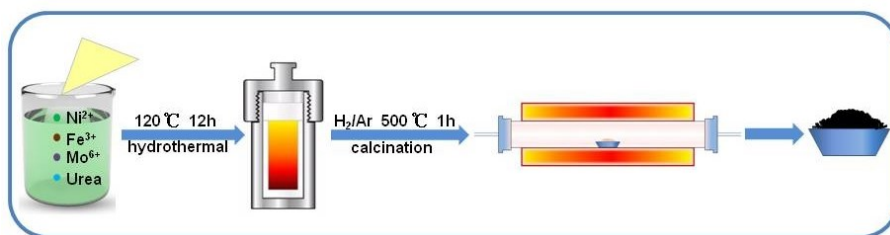
**Strong electronic coupled FeNi<sub>3</sub>/Fe<sub>2</sub>(MoO<sub>4</sub>)<sub>3</sub> nanohybrids for enhancing the electrocatalytic activity of oxygen evolution**

Zhaolong Wang,<sup>a</sup> Jian Bao,<sup>\*a</sup> Wenjun Liu,<sup>a</sup> Li Xu,<sup>a</sup> Yiming Hu,<sup>a</sup> Meili Guan,<sup>a</sup> Min Zhou,<sup>\*b</sup> and Huaming Li<sup>a</sup>

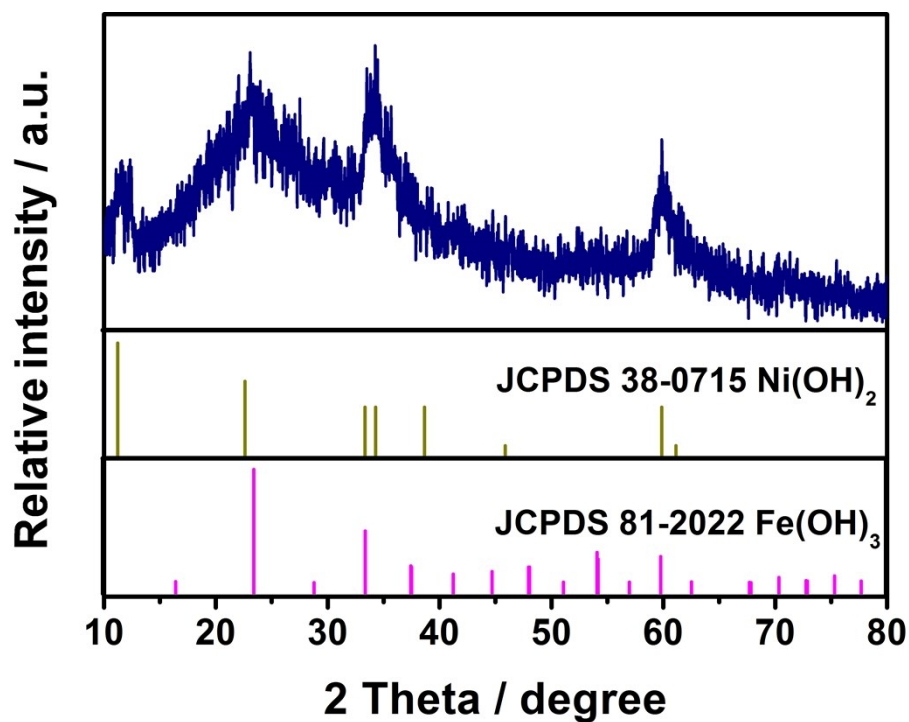
a. School of Chemistry and Chemical Engineering, Institute for Energy Research, Jiangsu University, Zhenjiang, Jiangsu, 212013, P. R. China.

b. Department of Applied Chemistry, School of Chemistry and Materials Science, University of Science and Technology of China (USTC), No. 96, Jinzhai Road, Hefei, Anhui, 230026, P.R. China.

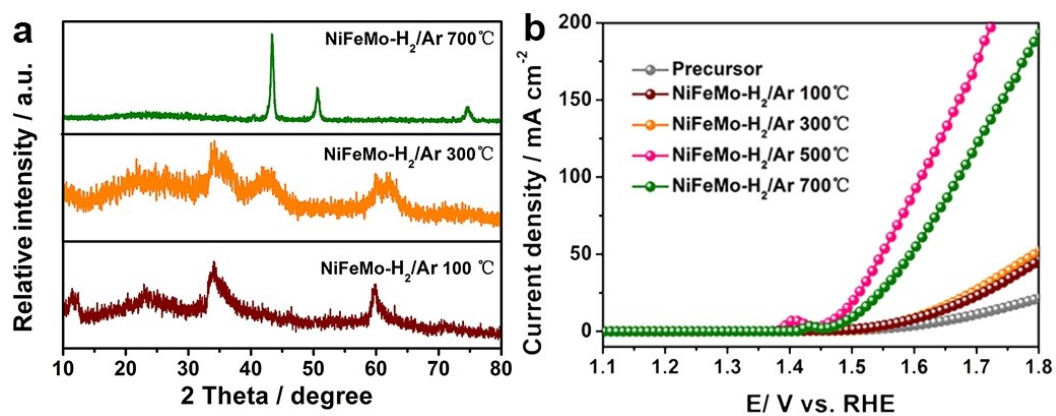
\*Correspondence: [baojian@ujs.edu.cn](mailto:baojian@ujs.edu.cn), [mzchem@ustc.edu.cn](mailto:mzchem@ustc.edu.cn)



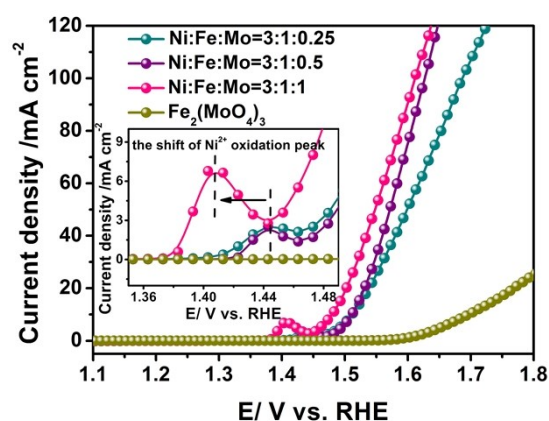
Supplementary Scheme. 1 Schematic illustration of the fabrication of  $\text{Fe}_2(\text{MoO}_4)_3/\text{FeNi}_3$  hybrid.



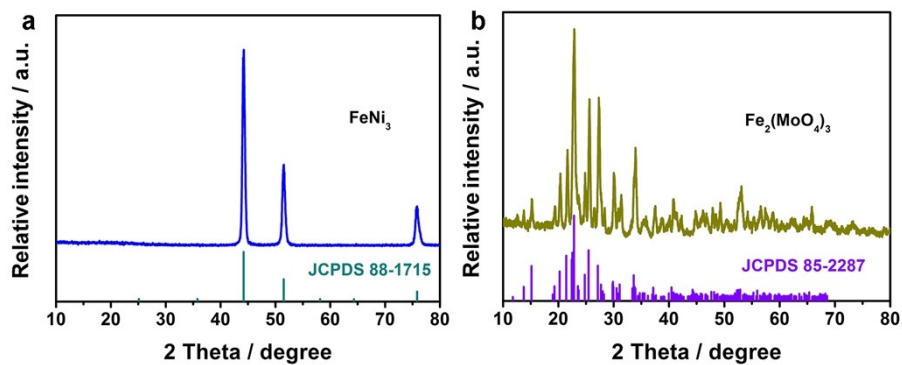
Supplementary Fig. 1 X-ray diffraction patterns of the NiFeMo precursor samples.



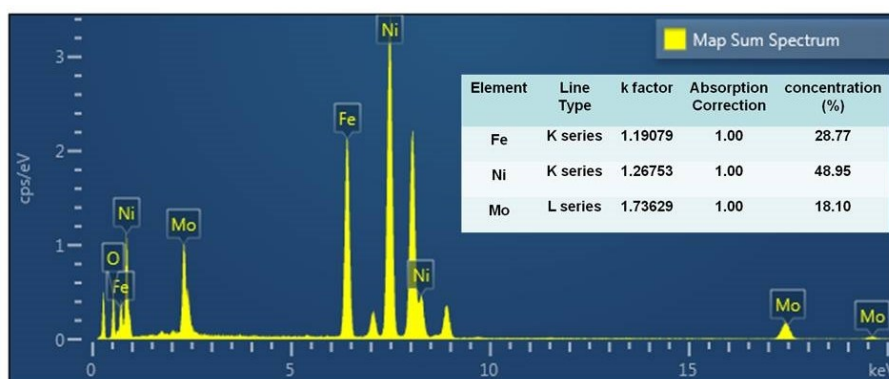
Supplementary Fig. 2 (a) Corresponding XRD patterns and (b) Polarization curves for OER of samples at different calcination temperatures.



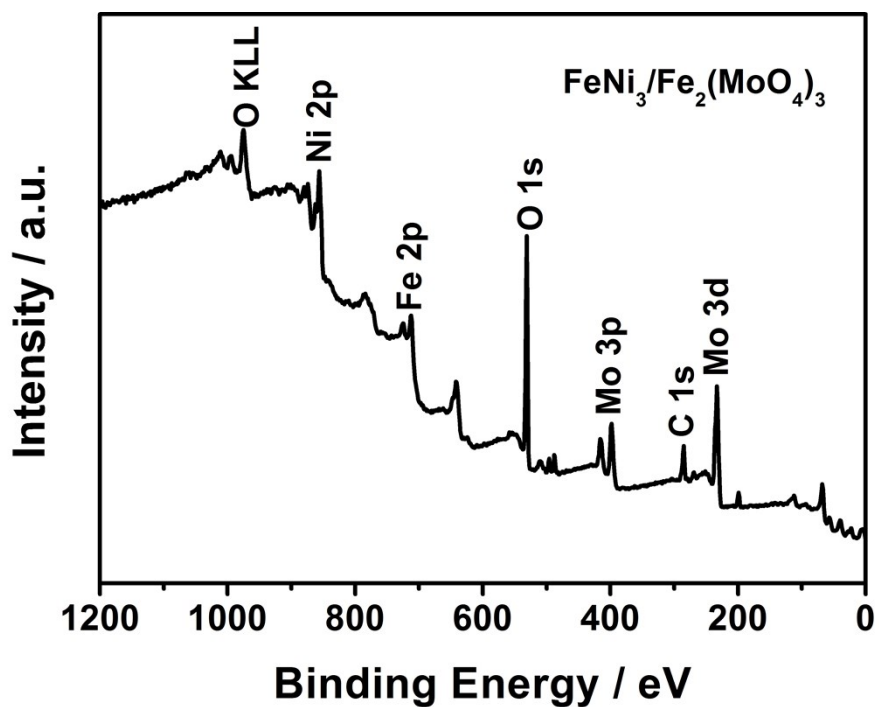
Supplementary Fig. 3 Polarization curves for OER of samples with different feed ratios.



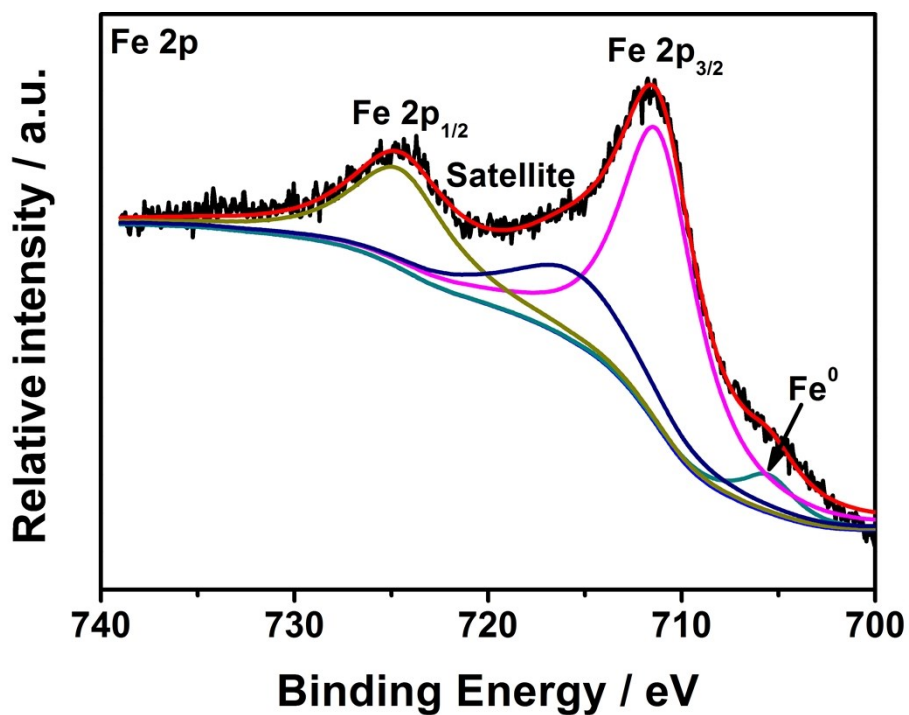
Supplementary Fig. 4 X-ray diffraction patterns of the FeNi<sub>3</sub> and Fe<sub>2</sub>(MoO<sub>4</sub>)<sub>3</sub> samples.



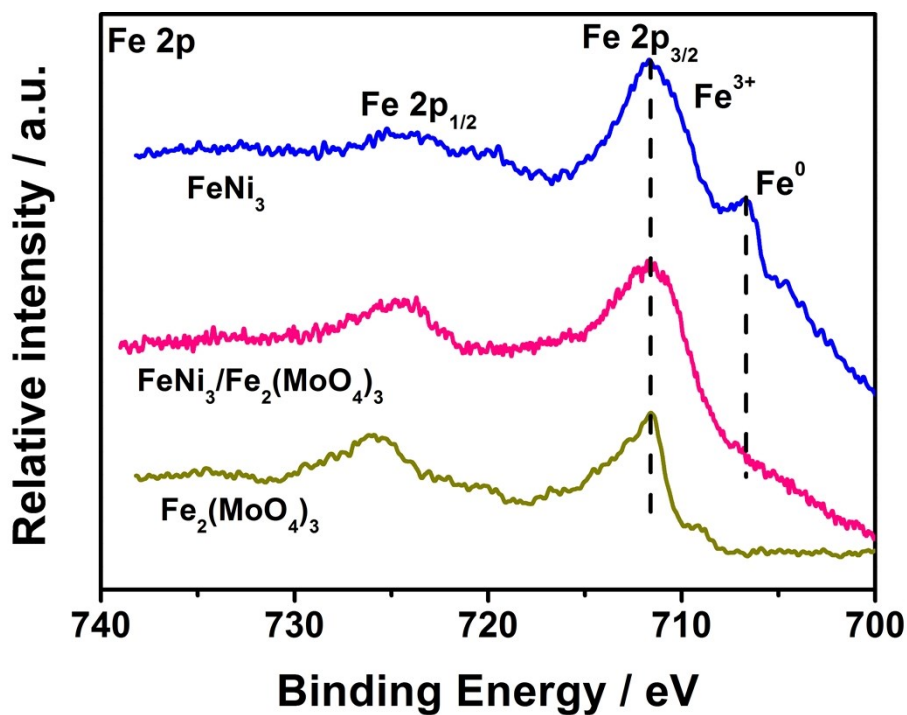
Supplementary Fig. 5 EDS spectrum of Fe<sub>2</sub>(MoO<sub>4</sub>)<sub>3</sub>/FeNi<sub>3</sub> hybrid catalyst.



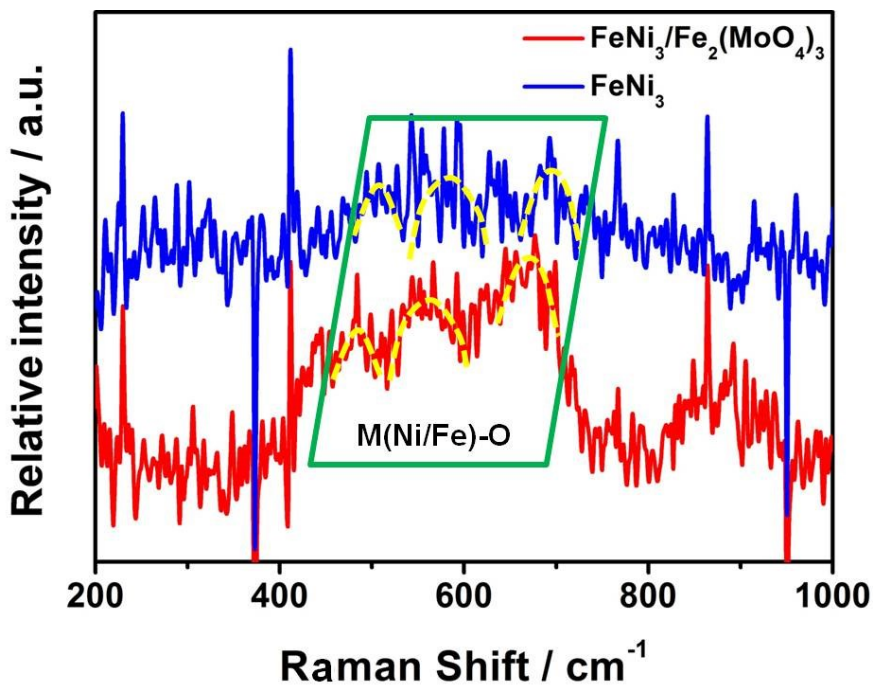
Supplementary Fig. 6 XPS survey spectrum of the  $\text{Fe}_2(\text{MoO}_4)_3/\text{FeNi}_3$  hybrid.



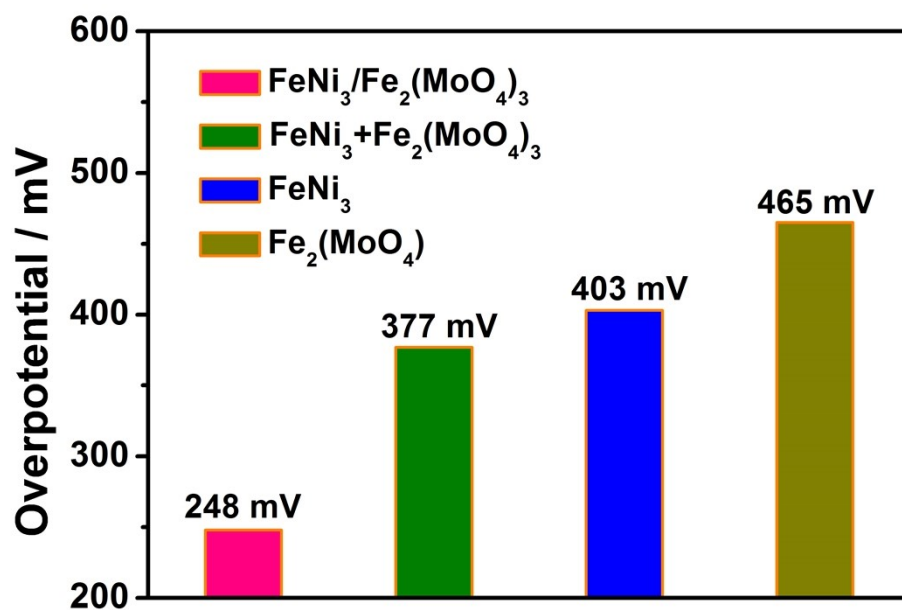
Supplementary Fig. 7 Fe 2p core-level spectra of  $\text{FeNi}_3/\text{Fe}_2(\text{MoO}_4)_3$  hybrid.



Supplementary Fig. 8 Fe 2p core-level spectra of FeNi<sub>3</sub> and Fe<sub>2</sub>(MoO<sub>4</sub>)<sub>3</sub> and FeNi<sub>3</sub>/Fe<sub>2</sub>(MoO<sub>4</sub>)<sub>3</sub> hybrid.



Supplementary Fig. 9 Raman spectra of FeNi<sub>3</sub> and FeNi<sub>3</sub>/Fe<sub>2</sub>(MoO<sub>4</sub>)<sub>3</sub> hybrid.

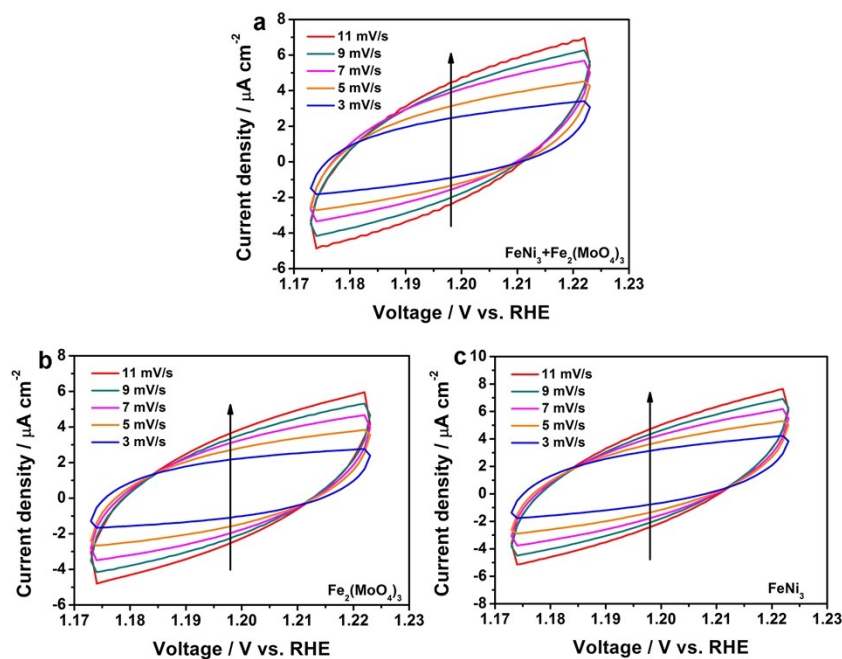


Supplementary Fig. 10 Comparison of the OER overpotential at 10 mA cm<sup>-2</sup> with a series of catalysts.

Supplementary Table 1 Electrocatalysis results of as-prepared  $\text{Fe}_2(\text{MoO}_4)_3/\text{FeNi}_3$  hybrid comparing with some state of the art catalytic electrodes.

Catalysts	Electrolyte	Overpotential at 10 mA.cm <sup>-2</sup>	Reference
$\text{FeNi}_3/\text{Fe}_2(\text{MoO}_4)_3$ hybrid	1 M KOH	248 mV	This work
CoFe LDH-Ar	1 M KOH	350 mV	[1]
$\text{FeNi}_3\text{N}$	1 M KOH	310 mV	[2]
Fe-CoOOH/G	1 M KOH	330 mV	[3]
$\text{NiCoO}_x$	1 M KOH	336 mV	[4]
$\text{Fe}_2\text{P}/\text{Fe}_4\text{N}@N\text{-C}$	1 M KOH	410 mV	[5]
$\text{FeNi}_3@NC$	1 M KOH	277 mV	[6]
$\text{FeNi}_3\text{-Fe}_3\text{O}_4$ NPs/MOF-CNT	1 M KOH	234 mV	[7]
$\text{FeNi}_3$ -modified $\text{Fe}_2\text{O}_3/\text{NiO}/\text{MoO}_2$	1 M KOH	282 mV	[8]
$\text{FeNi}_3\text{N}/\text{FeNi}_3$	1 M KOH	254 mV	[9]
$\text{FeNiF}/\text{NCF}$	1 M KOH	260 mV	[10]



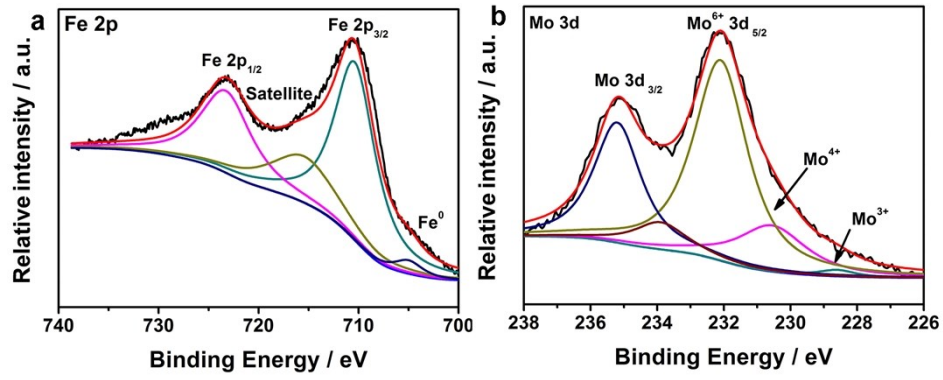


Supplementary Fig. 11 CV curves of a)  $\text{Fe}_2(\text{MoO}_4)_3 + \text{FeNi}_3$ , b)  $\text{Fe}_2(\text{MoO}_4)_3$ , c)  $\text{FeNi}_3$  at different scan rates from 3 to 11 mV/s between 1.17 V and 1.23 V vs. RHE in 1.0 M KOH.

Supplementary Table 2 Impedance fitting results of as-prepared  $\text{Fe}_2(\text{MoO}_4)_3/\text{FeNi}_3$  hybrid samples comparing with different catalytic electrodes.

Samples	$R_s / \Omega$	$C_{dl} / \text{F}$	$R_{ct} / \Omega$
$\text{Fe}_2(\text{MoO}_4)_3$	8.402	$2.914 \times 10^{-6}$	415.5
$\text{FeNi}_3$	8.866	$3.692 \times 10^{-6}$	192.58
$\text{Fe}_2(\text{MoO}_4)_3/\text{FeNi}_3$	7.069	$3.923 \times 10^{-6}$	9.53
$\text{Fe}_2(\text{MoO}_4)_3 + \text{FeNi}_3$	8.923	$1.101 \times 10^{-5}$	108

Notes:  $R_s$  value is used to describe the resistance of solution;  $C_{dl}$  values are the double-layer capacitance;  $R_{ct}$  represents the resistances of charge transfer.



Supplementary Fig. 12 High-resolution XPS spectra for Fe 2p and Mo 3d region of the  $\text{Fe}_2(\text{MoO}_4)_3/\text{FeNi}_3$  hybrid after OER.

## References:

- [1] Y. Wang, Y. Zhang, Z. Liu, C. Xie, S. Feng, D. Liu, M. Shao, S. Wang, Layered double hydroxide nanosheets with multiple vacancies obtained by dry exfoliation as highly efficient oxygen evolution electrocatalysts, *Angew. Chem. Inter. Edit.*, 2017, **56**, 5867-5871.
- [2] X. Jia, Y. Zhao, G. Chen, L. Shang, R. Shi, X. Kang, G. I. N. Waterhouse, L. Wu, C. Tung, T. Zhang, Ni<sub>3</sub>FeN Nanoparticles Derived from Ultrathin NiFe-Layered Double Hydroxide Nanosheets: An Efficient Overall Water Splitting Electrocatalyst, *Adv. Energy Mater.*, 2016, **6**, 1502585.
- [3] X. Han, C. Yu, S. Zhou, C. Zhao, H. Huang, J. Yang, Z. Liu, J. Zhao, J. Qiu, Ultrasensitive Iron-Triggered Nanosized Fe-CoOOH Integrated with Graphene for Highly Efficient Oxygen Evolution, *Adv. Energy Mater.*, 2017, **7**, 1602148.
- [4] X. Deng, S. Öztürk, C. Weidenthaler, H. Tüysüz, Iron-induced activation of ordered mesoporous nickel cobalt oxide electrocatalyst for the oxygen evolution reaction, *ACS Appl. Mater. Inter.*, 2017, **9**, 21225-21233.
- [5] X. Fan, F. Kong, A. Kong, A. Chen, Z. Zhou, Y. Shan, Covalent porphyrin framework-derived Fe<sub>2</sub>P@Fe<sub>4</sub>N-coupled nanoparticles embedded in N-doped carbons as efficient trifunctional electrocatalysts, *ACS Appl. Mater. Inter.*, 2017, **9**, 32840-32850.
- [6] D. Chen, J. Zhu, X. Mu, R. Cheng, W. Li, S. Liu, Z. Pu, C. Lin, S. Mu, Nitrogen-Doped carbon coupled FeNi<sub>3</sub> intermetallic compound as advanced bifunctional electrocatalyst for OER, ORR and zn-air batteries, *Appl. Cataly. B-Environ.*, **2020**, 268, 118729.
- [7] K. Srinivas, Y. Lu, Y. Chen, W. Zhang, D. Yang, FeNi<sub>3</sub>-Fe<sub>3</sub>O<sub>4</sub> Heterogeneous Nanoparticles Anchored on 2D MOF Nanosheets/1D CNT Matrix as Highly Efficient Bifunctional Electrocatalysts for Water Splitting, *ACS Sustain. Chem. Eng.*, **2020**, 8, 3820-3831.
- [8] X. Zhang, Y. Chen, M. Chen, B. Wang, B. Yu, X. Wang, W. Zhang, D. Yang, FeNi<sub>3</sub>-modified Fe<sub>2</sub>O<sub>3</sub>/NiO/MoO<sub>2</sub> heterogeneous nanoparticles immobilized on N, P co-doped CNT as an efficient and stable electrocatalyst for water oxidation, *Nanoscale* **2020**, 12, 3777-3786.
- [9] X. Fu, J. Zhu, B. Ao, X. Lyu, J. Chen, Enhanced oxygen evolution reaction activity of FeNi<sub>3</sub>N nanostructures via incorporation of FeNi<sub>3</sub>, *Inorg. Chem. Commun.*, **2020**, 113, 107802.
- [10] M. Zha, C. Pei, Q. Wang, G. Hu, L. Feng, Electrochemical oxygen evolution reaction efficiently boosted by selective fluoridation of FeNi<sub>3</sub> alloy/oxide hybrid, *J. Energy Chem.*, **2020**, 47, 166-171.